

2012년 8월

박사학위 논문

Specification of the  
Lateral Calcaneal Coordinate  
System for the Screw Fixation  
of Calcaneal Fracture

조 선 대 학 교 대 학 원

의 학 과

김 정 호

# Specification of the Lateral Calcaneal Coordinate System for the Screw Fixation of Calcaneal Fracture

종골골절의 나사못 고정을 위한  
외측종골좌표계의 설정법

2012년 8월 24일

조 선 대 학 교    대 학 원

의    학    과

김    정    호

# Specification of the Lateral Calcaneal Coordinate System for the Screw Fixation of Calcaneal Fracture

지도교수 이 상 홍

이 논문을 의학 박사학위신청 논문으로 제출함

2012년 4월

조 선 대 학 교 대 학 원

의 학 과

김 정 호

## 김정호의 박사학위 논문을 인준함

위원장    조선대학교                      교    수    하상호 (인)

위    원    조선대학교                      교    수    이상홍 (인)

위    원    대구가톨릭대학교    조교수    이연수 (인)

위    원    조선대학교                      교    수    문영래 (인)

위    원    조선대학교                      부교수    이준영 (인)

2012년    06월

조 선 대 학 교    대 학 원

# CONTENTS

ABSTACT-----	v
I . INTRODUCTION-----	1
II . MATERIALS and METHODS-----	3
III . RESULTS-----	7
IV . DISCUSSION-----	8
V . CONCLUSIONS-----	13
REFERENCES-----	14

# LIST OF TABLES

Table 1. Interobserver differences in the location of the origin and angular alignment of the lateral coordinate system ----- 16

Table 2. Interobserver differences in the safe screw angle measurements ----- 17

Table 3. Inferior and superior limits of the safe screw insertion direction ----- 18

# LIST OF FIGURES

Fig. 1. The lateral-to-medial screw insertion treatment for the Sander Type II calcaneal fracture -----	19
Fig. 2. Medial view of the ankle which shows complex structure -----	20
Fig. 3. The 3D polygon models of the talus and calcaneus---	21
Fig. 4. Three prominent points were specified on the lateral calcaneal bony plane. Prominence was identified in the inferior view -----	22
Fig. 5. The minimal lateral calcaneal plane was determined by the 3 prominent points on a small area near to talocalcaneal joint -----	23

Fig. 6. Definition of the lateral calcaneal coordinate system	24
Fig. 7. The measured angles ( $\theta$ and $\phi$ ) in the safe screw insertion simulation where the screw's diameter was set as 6.5 mm	25
Fig. 8. Safe zone for the screw insertions the angle between the superior and inferior limits	26
Fig. 9. Superior and inferior limits in the quasi-anteversion ( $\theta$ ) of the safe screw insertion direction	27
Fig. 10. Superior and inferior limits in the quasi-infraversion ( $\phi$ ) of the safe screw insertion direction	28
Fig. 11. A schematic comparison of the MIS lateral calcaneal plane and the extensive lateral calcaneal plane	29



# ABSTRACT

## 종골골절의 나사못 고정을 위한 외측종골좌표계의 설정법

김 정 호

지도교수 : 이 상 홍

조선대학교 대학원 의학과

**목적:** 관절내 종골 골절의 최소 침습적 내고정술 시 외측에서 내측의 재거돌기의 방향으로 외측에서 내측의 재거돌기 방향으로 나사를 삽입하여 고정하는 종골의 외측 관절면과 재거돌기를 고정하는 과정은 아주 중요한 골절 정복 과정의 일부이다. 이 방법은 관절내 종골 골절의 수술적 치료중 필수적으로 고정을 하여야 하나 수술실에서 C형 방사선 투과기를 사용한다 하더라도 많은 시간이 걸리고 종골 내측을 지나가는 인대, 신경에 손상을 주기 쉽다. 또한 나사못의 삽입시 거골하 관절을 침범할 가능성이 높아 안전하게 나사못을 고정하는 것은 어려운 방법이다. 이에 관절내 종골 골절의 재거 돌기 고정에 있어서 외측-내측 재거 돌기나사 삽입을 3차원적으로 안전한 방향으로 삽입할 수 있는 나사 유도기구에 대한 연구가 필요하다. 본 논문은 안전하게 재거돌기 나사 방향을 규명하고 유도하는데 있어 기본 지형이 되는 외측 종골 좌표계의 설정에 있어 반복성 및 재현성을 확보할 수 있는 방법에 대한 해부학적 분석과 설정법을 개발하고자 하였다.

**대상 및 방법:** 보관되어 있는 CT 영상정보 DB로부터 정상인 종골을 골라서 컴퓨터 CAD모델로 재건하였다. 이 재건된 모델에서 안전한 나사위치와 삽입각도를 시뮬레이션을 통하여 안전한 나사 방향을 측정하였다. 안전한 나사 방향을 측정하기

위해서는 종골의 외측면에 기반을 둔 평면과 좌표계를 정의하여야 하였다. 거골하 관절의 외측선에서 10 mm 내외의 거리에서 튀어나온 뼈의 해부학적 위치점을 기반으로 하여 외측평면을 정의하고, 이평면과 거골/종골의 외측관절선 벡터를 이용하여 외측 종골좌표계를 지정하는 방법을 개발하였다. 본 연구에서 제시된 외측 종골좌표계 지정법과 이를 기준으로 한 외측-내측 나사못삽입을 위한 안전나사각도를 측정하였다. 외측종골좌표계의 측정자간 신뢰성은 CT촬영 시에 생성된 좌표계에 대한 지정된 외측종골좌표계의 원점의 위치와 좌표계의 회전각에 있어 측정자간 측정값의 차이로 평가하였다. 안전한 나사방향의 측정자간 신뢰성은 내측의 안전나사방향의 상측한계와 하측한계가 보이는 각도 값에 있어 측정자간의 편차로 계산하였다. 총 20개의 거골/종골 3차원모델을 이용한 나사못삽입 안전영역의 상방한계와 하방한계의 방향을 측정하였고, 이 두 한계방향의 중간 값을 최종적으로 도출하였다.

**결과:** 좌표원점 지정의 신뢰성에서 가장  $0.5 \pm 0.6$  mm 였고, 좌표계의 정렬각도의 신뢰성은  $2.0 \pm 3.3^\circ$  로 측정되었다. 안전나사방향의 지정법의 측정자간 신뢰성은 준전향회전각 측정에서는  $1.0 \pm 1.4^\circ$  , 준하향회전각 측정에서는  $1.1 \pm 2.4^\circ$  을 보였다. 총 20개의 거골/종골 3차원모델을 이용한 안전나사못삽입영역 측정에서 준전향회전각은 하방한계가  $15.1 \pm 4.3^\circ$  상방한계가  $11.3 \pm 5.7^\circ$  였다. 준하향회전각은 하방한계가  $9.8 \pm 4.8^\circ$  상방한계가  $-8.3 \pm 4.6^\circ$  였다. 상방한계방향과 하방한계방향의 중간위치는 결과적으로 준전향회전각은  $13.2 \pm 4.9^\circ$  , 준하향회전각은  $0.7 \pm 4.4^\circ$  로 나타났다.

**결론:** 종골 골절의 치료에 있어서 최근에 최소 침습 수술이 많이 행해지고 있음을 감안할 때, 안전한 재거 돌기 나사의 고정을 위해서는 거골하 관절면 근처의 종골의 외측돌출부를 기반으로 종골 외측좌표계 지정 및 안전나사삽입측정법은 재현성에서 좋은 결과를 보였다.

# I . INTRODUCTION

Calcaneal fracture is the most frequently fractured tarsal bone comprising 65% of tarsal injuries,<sup>1)</sup> especially they most commonly occur in a young, working subset of the population, resulting in a large economic impact.<sup>2-4)</sup>

The lateral-to-medial screw insertion fixation has been widely performed as a surgical treatment of calcaneal fractures (Fig. 1). However, a little amount of malalignment of the screw insertions may harm and may create new injury in ligaments, nerves, or subtalar articulation. A safe screw insertion being able to avoid those unwanted problems is difficult to be achieved because of limited vision during surgery and anatomical complexity of the talocalcaneal joint.<sup>5,6)</sup> Even a C-arm X-ray scanner cannot provide surgeon 3-dimensionally confirmation of invasion-free screw insertion due to its limitation of 2D view and occlusion of anatomic features.

In medial opening of the sustentaculum tali, the posterior tibial tendon sheath is shown over the sustentaculum tali and the flexor digitorum longus tendon is seen posteriorly (Fig. 2).<sup>7)</sup> Hence the screw should not be inserted up to over the medial surface of the sustentaculum tali.

The lateral-to-medial screw fixation has been widely performed as a surgical treatment of calcaneal fractures. However, a little amount of malalignment of the screw insertions may harm and create new injury in ligaments, nerves, or subtalar articulation. A safe screw insertion being avoiding those unwanted problems is difficult to be achieved because of

limited field of view during surgery and anatomical complexity of the talocalcaneal joint. Even a C-arm X-ray scanner cannot provide the surgeon 3-dimensionally confirmation of invasion-free screw insertion due to its limitation of 2D view and occlusion of anatomic features.

Therefore, to increase the safe screw insertion rate, the safe screw insertion direction has to be identified quantitatively so that it does not harm surrounding tissues and articulation.<sup>8-10)</sup> To this end, a local coordinate system, i.e. as a base datum, on the lateral calcaneal surface should be specified in repeatable manner. To my best knowledge, there has not been any protocol for specification of the local coordinate system or the measurement of safe insertion directions.

Hence, the current study aims to develop a lateral calcaneal coordinate system which can be used as a guide specified for the minimal invasive surgery, and to assess the safe screw insertion angle with respect to the local coordinate system.

## II . MATERIALS and METHODS

### **Materials:**

For the 20 ankle without fracture or abnormal deformity in the calcaneus, 3-dimensional (3D) anatomic analysis was performed. This study included samples from 17 males and 3 females with mean  $42.7 \pm 18.9$  years old. Computed tomography (CT) images of the ankle were extracted from database of the Chosun University hospital. The CT images were converted into DICOM (The Digital Imaging and Communications in Medicine) file after performing an image processing of a standard algorithm. The CT images were taken with a slice thickness of 1.25 mm, the field of view of 200 mm, and 512x512 resolutions.

### **3D reconstruction of the talus and calcaneus:**

For reconstruction of 3D bone models, the DICOM files were imported to Mimics v13.1 (Materialise, Belgium). The bony contour was initially automatically segmented by Hounsfield Unit (HU) 225, and final segmentation was completed through combination of automatic and manual works. The final models of the bones were 3D polygon models (Fig. 3).

### **Specification of the lateral calcaneal plan:**

The STL format files of the polygon models, created in Mimics, were imported into Rapidform 2006 (INUSTECH, Seoul, Korea). Bony landmarks, lateral plane, and coordinate system on the lateral calcaneus were specified

and determined using Rapidform. In the inferior view of the lateral calcaneal bony surface posterior to talocalcaneal joint, 3 prominent points (p1, p2, and p3 in Fig. 4) were identified such that the 3 points are placed in a line. Two of the 3 points were specified in the superior and the third one in the inferior (Fig. 5).

A lateral calcaneus plane was defined on as the triangle whose area includes the 3 prominent points required to define a calcaneus plan (Fig. 5).

### **Specification of the lateral calcaneal coordinate system:**

A lateral calcaneal coordinate system was specified based on the lateral calcaneal plane. To define the first coordinate, the superiormost (P4) and inferiormost (P5) calcaneal points along talocalcanal articulation line on the minimal calcaneal plane view were specified (Fig. 6). Then the 2 points were projected onto the lateral plane (i.e.,  $P4 \rightarrow P4'$  ,  $P5 \rightarrow P5'$  in Fig. 5), and the line  $\overline{P_4'P_5'}$  connecting  $P4'$  and  $P5'$  was bisected. The line  $\overline{P_4'P_5'}$  was assigned as a parallel line to Y-axis of the lateral calcaneus coordinate system to be defined. A point which is 5 mm posterior to P6 and normal  $\overline{P_4'P_5'}$  was assigned as the origin (0) of the lateral calcaneal coordinate system. The extended vector from the line  $\overline{P_6O}$  became X-axis, and Y-axis as the vector parallel to  $\overline{P_4'P_5'}$  . Z-axis is automatically determined by the cross product of the unit vectors of the X-axis and Y-axis. The reason why the origin was placed at the point 0 comes from the fact that it is practically

used as the inlet of lateral-to-medial screw insertion treatment.

### Simulation of the lateral-to-medial safe screw insertion:

The lateral-to-medial screw fixation for calcaneal fracture was simulated to assess the safe screw insertion direction. From the point 0, a screw of diameter 6.5 mm was virtually inserted toward sustentaculum tali. There were 2 conditions built to restrict the screw location on the sustentaculum tali, they are follows.

#### *Two conditions for the safe screw insertion*

*Condition 1. The distal end of a screw should be placed within medial eminence of the sustentaculum tali*

*Condition 2. The screw should not invade talocalcaneal articulation surface.*

Keeping the 2 conditions, safe screw insertion direction was measured in terms of two angles (  $\theta$  D\_Dd\_\_\_\_\_Áá88\_\_\_\_\_

\_\_\_\_\_ is the angular deviation of the screw axis from XZ plane in the X-axis view. The safe screw insertion direction ranges from the superior limit to the inferior limit as Fig. 8. The region encompassing the 2 limits are the safe screw insertion zone.

### **Reproducibility of the safe screw insertion direction measurement:**

To test the fidelity of the screw insertion direction measurement, a reproducibility (interobserver reliability) test was performed. The tested quantities for this test were angles  $\theta$  \_\_\_ for the inferior limit and the superior limit, and the location of the origin and angular alignment of the coordinate system. As in the reproducibility test of the local coordinate system definition, each observer measured 10 feet models (i.e., specimen 1-10 in Table 2). To evaluate reproducibility, interobserver difference by 2 observers was measured for each quantity.



### III . RESULTS

#### Reproducibility of the local coordinate system definition (Table 1):

The largest interobserver difference in the location of the origin was  $0.5 \pm 0.6$  mm for the Y-coordinate. And the largest interobserver difference in the angular alignment of the lateral coordinate system was  $2.0 \pm 3.3^\circ$  for the rotation of the lateral coordinate system about Z-axis of the global coordinate system.

#### Reproducibility of the screw insertion direction measurement (Table 2):

The largest interobserver difference in the angle measurements for the angle  $\Theta$  was observed at the superior limit direction, which was  $1.0 \pm 1.4^\circ$  .

In the measurement of  $\phi$  D\_Dd\_\_\_\_\_ \_\_\_\_\_

D\_Dd\_\_\_\_\_ \_\_\_\_\_

#### The safe screw insertion direction (Table 3):

The inferior and superior limits of  $\Theta$  were  $15.1 \pm 4.3^\circ$  and  $11.3 \pm 5.7^\circ$  , respectively, while the inferior and superior limits of  $\phi$  were  $9.8 \pm 4.8^\circ$  and  $-8.3 \pm 4.6^\circ$  (or  $8.3 \pm 4.6^\circ$  in absolute), respectively. The central direction as the middle of the safe superior and inferior screw insertion directions was  $\Theta = 13.2 \pm 4.9^\circ$  and  $\phi = 0.7 \pm 4.4^\circ$  .

## IV. DISCUSSION

The current study developed a lateral calcaneal coordinate system based on a minimal bony region and a talocalcaneal articulation line. More importantly, the safe screw insertion direction for lateral-to-medial screw insertion treatment was assessed from 20 normal Korean ankle. The safe screw insertion direction data will be critical clue for safe surgery and development of a screw guiding device.

Based on the founding of the current study, a design of screw guiding device for the safe lateral-to-medial screw fixation can be targeted from the central direction angles. The angles

D\_Dd\_\_\_\_\_

\_\_\_\_\_ plane of the lateral calcaneal coordinate system) for quasi-anteversion angle measurement is a little bit dorsiflexed. This is true for the quasi-infraversion whose baseline direction (or ZX plane of the lateral calcaneal coordinate system) is a little bit everted. The quasi-anteversion is larger for the inferior safe insertion limit direction than for the superior limit direction (Fig. 9). Also, the quasi-infraversion is larger for the inferior safe insertion limit direction (Fig. 10). In practical design of a screw guiding device, targeted safe angles can be concisely determined

as  $\Theta = 13^\circ$  and  $\Phi = 00$  from the central direction angles, i.e.  $\Theta = 13.2 \pm 4.9^\circ$  and  $\Phi = 0.7 \pm 4.4^\circ$ .

There have been various treatment algorithms for calcaneus fractures with little consensus beyond the debilitating deformity that results from the fracture.<sup>11)</sup> For the purpose of preventing such deformities, various screw fixation techniques for calcaneal fracture have been used, such single screw insertion, dual screw insertion and poly-axially locked plate screws.<sup>12)</sup> For comminuted calcaneal fractures, subtalar arthrodesis or poly-axially locked plate screws can be a good treatment.<sup>13)</sup> Another clinical study supports that percutaneous fixation is a reasonable alternative for moderately displaced Type II fractures provided adequate control over anatomic joint reduction with either subtalar arthroscopy or high-resolution (3-D) fluoroscopy.<sup>10)</sup> Osteosynthesis using screws or plate-screw fixations for Sanders Type II or III fracture showed excellent clinical results.<sup>14)</sup>

Classification systems of intraarticular fractures of the calcaneus are well documented in Daftary et al.'s study.<sup>5)</sup> The two major systems for classifying calcaneal fractures include the Hannover and Sanders classifications<sup>5,15)</sup>. The Hannover classification assigns one point to each of a possible five fragments and one point to involvement of each of three articular surfaces<sup>5)</sup>. The Sanders classification is used more commonly and is based on the pathophysiology proposed by Soeur and Remy; it relies on sagittally reconstructed CT images reformatted parallel and perpendicular to the posterior facet of the subtalar joint. Type I fractures are nondisplaced<sup>5,15)</sup>. Type II fractures (two articular pieces) involve the

posterior facet and are subdivided into types A, B, and C, depending on the medial or lateral location of the fracture line (more medial fractures are harder to visualize and reduce intraoperatively). Type III fractures (three articular pieces) include an additional depressed middle fragment and are subdivided into types AB, AC, and BC, depending on the position and location of the fracture lines. Type IV fractures (four or more articular fragments) are highly comminuted (Fig. 11). The Sanders classification has been shown to have good interobserver variability, making it useful in clinical practice<sup>15)</sup>. The Sanders classification system is useful not only in treatment planning but in helping to determine prognosis.<sup>15)</sup> In their series of 120 intraarticular calcaneal fractures, type I fractures were treated without surgery.<sup>15)</sup> Patients with type II and type III fractures who underwent surgery experienced excellent or good clinical results in 73% and 70% of cases, respectively.<sup>15)</sup>

However, Talus, calcaneus, and talocalcaneal joint have very complicated articulation anatomy.<sup>16,17)</sup> The calcaneus, the largest tarsal bone specifically designed to support the body and endure a great degree of force, and the most common tarsal bone to be fractured is the calcaneus, and calcaneal fractures account for about 1%-2% of all fractures.<sup>5)</sup> And these fractures typically occur because of axial loading in men 30-60 years old and usually have poor outcomes<sup>5)</sup>. The talus and the calcaneus share the bulk of load transmitted from the leg to the skeleton of the foot, have close inter-relationship according to the articular surface contact conditions and the morphology of the talus and the calcaneus.<sup>6)</sup> The sustentaculum tali of the calcaneus is

situated immediately below and medial to the neck of the talus and thus the superior articular surface of the talus, the neck of the talus and the sustentaculum tali are situated in the same vertical plane.<sup>6)</sup> Mahato et al. said that the load received at the upper surface of the talus splits into two vectors inferiorly, and though the neck of the talus is subjected to great compressive stress, a large percentage of the load does not reach up to the upper surface of the sustentaculum tali.<sup>6)</sup> For this reason, there are many things to be kept in mind when screws are inserted in this area. The medial and inferior calcaneal nerves should not be harmed by the screw fixation.<sup>18)</sup>

The lateral calcaneal plane of the current study can be adopted for the minimal invasive surgery since the triangular plane defined by 3 near-articulation prominences can be revealed in spite of minimal opening size. In this sense the calcaneal lateral plane can be called the minimal invasive surgery (MIS) lateral coordinate plane (Fig. 11). In contrast, if a lateral calcaneal plane is defined by prominences throughout the whole lateral calcaneal bony surface, it can be called the extensive lateral calcaneal plane.

The protocols for determination of the MIS lateral coordinate system and the safe screw direction were proposed and had an excellent interobserver reliability. The largest interobserver difference in the location of the origin was  $0.5 \pm 0.6$  mm and the largest interobserver difference in the angular alignment of the lateral coordinate system was  $2.0 \pm 3.3^\circ$ . The largest interobserver differences in the angle measurements were  $1.0 \pm 1.4^\circ$  and  $1.1 \pm 2.4^\circ$ , respectively for the angle  $\theta$  and

□\_ô\_\_\_\_\_타\_\_\_\_\_ô\_\_\_\_\_타\_\_\_\_\_ô\_\_\_\_\_

The current study has its limitations. First the measurements did not consider the effects of soft tissues that will affect stability in identifying bony prominences. And thickness of soft tissue may also slightly change the lateral calcaneal plan. The consideration of soft tissue is only investigated through cadaveric measurements. Furthermore the number of specimens was 20 and is not sufficient to represent anatomic variations.

Future advance of the current study is being planned. The number of specimen could be measured. And a new screw guiding plate with application of the founding will be developed. And with the guiding plate clinical validity will be assessed. Based on some amount of clinical and anatomical assessment, an indication of the guiding plate can be figured out in terms of feasible anatomic dimension and fracture types.

## V. CONCLUSIONS

The current study developed a lateral calcaneal coordinate system based on a minimal bony region and a talocalcaneal articulation line. The safe lateral-to-medial screw insertion direction was  $\Theta=13.2^\circ$  and  $\phi=10.4^\circ$  referred to the MIS lateral calcaneal plane.

The protocols for determination of the MIS lateral coordinate system and the safe screw direction were proposed and showed very excellent interobserver reliability.

From this study, the authors believe a guiding system for inserting screw for the fixation of comminuted calcaneal fracture can be developed. And the protocols for determining the lateral coordinate system and the safe screw direction will play a key role in ankle related surgical devices, especially in development of navigation-assisted ankle surgery system.

## REFERENCES

1. Lindsay W, Dewar F. Fractures of the os calcis. *Am J Surg.* 1958;95:555-76.
2. Sanders R. Displaced intra-articular fractures of the calcaneus. *J Bone Joint Surg Am.* 2000;82:225-50.
3. Sohn H-M, Ha S-H, Lee S-H, Lee J-Y, Kim J-H, Lee S-J. Treatment of Intra-articular Calcaneal Fractures Using Minimally Invasive Sinus Tarsi Approach in Diabetic Patients. *Journal of the Korean Fracture Society.* 2008;21:195-9.
4. Kim S-T, Youn T-H, Park J-B, Lee J-Y. Surgical Outcomes of Intra-articular Fractures of Calcaneus using AO Calcaneal Plate. *J Korean Foot Ankle Soc.* 2009;13:75-9.
5. Daftary A, Haims AH, Baumgaertner MR. Fractures of the calcaneus: a review with emphasis on CT. *Radiographics.* 2005;25:1215-26.
6. Mahato NK. Morphology of sustentaculum tali: Biomechanical importance and correlation with angular dimensions of the talus. *Foot (Edinb).* 2011;21:179-83.
7. Della Rocca GJ, Nork SE, Barei DP, Taitzman LA, Benirschke SK. Fractures of the sustentaculum tali: injury characteristics and surgical technique for reduction. *Foot Ankle Int.* 2009;30:1037-41.
8. Macey LR, Benirschke SK, Sangeorzan BJ, Hansen ST. Acute Calcaneal Fractures: Treatment Options and Results. *J Am Acad Orthop Surg.* 1994;2:36-43.
9. Mauffrey C, Bailey JR, Hak DJ, Hammerberg ME. Percutaneous reduction and fixation of an intra-articular calcaneal fracture using an inflatable bone



- tamp: description of a novel and safe technique. *Patient Saf Surg.* 2012;6:6.
10. Rammelt S, Amlang M, Barthel S, Gavlik JM, Zwipp H. Percutaneous treatment of less severe intraarticular calcaneal fractures. *Clin Orthop Relat Res.* 2010;468:983–90.
11. Reddy V, Fukuda T, Ptaszek AJ. Calcaneus malunion and nonunion. *Foot Ankle Clin.* 2007;12:125–35.
12. Richter M, Droste P, Goesling T, Zech S, Krettek C. Polyaxially-locked plate screws increase stability of fracture fixation in an experimental model of calcaneal fracture. *J Bone Joint Surg Br.* 2006;88:1257–63.
13. Buch BD, Myerson MS, Miller SD. Primary subtalar arthrodesis for the treatment of comminuted calcaneal fractures. *Foot Ankle Int.* 1996;17:61–70.
14. Jain V, Kumar R, Mandal DK. Osteosynthesis for intra-articular calcaneal fractures. *J Orthop Surg (Hong Kong).* 2007;15:144–8.
15. Sanders R, Fortin P, DiPasquale T, Walling A. Operative treatment in 120 displaced intraarticular calcaneal fractures. Results using a prognostic computed tomography scan classification. *Clin Orthop Relat Res.* 1993;290:87–95.
16. Mahato NK, Murthy SN. Articular and angular dimensions of the talus: Inter-relationship and biomechanical significance. *Foot (Edinb).* 2012;22:85–9.
17. Palma Ld, Santucci A, Ventura A, Marinelli M. Anatomy and embryology of the talocalcaneal joint. *Foot and Ankle Sur.* 2003;9:7–18.
18. Louisia S, Masquelet AC. The medial and inferior calcaneal nerves: an anatomic study. *Surg Radiol Anat.* 1999;21:169–73.

**Table 1.** Interobserver differences in the location of the origin and angular alignment of the lateral coordinate system.

#	Interobserver difference					
	Location of the origin (mm)			Angular alignment of the lateral coordinate system about the global coordinate system ( ° )		
	x	y	z	X-axis	Y-axis	Z-axis
1	-0.3	-0.6	0.0	-0.7	0.0	-2.7
2	0.4	1.1	-1.8	-1.5	0.2	4.7
3	0.0	0.2	-0.5	-0.5	-0.7	2.7
4	0.3	0.5	0.3	-3.5	0.9	2.2
5	0.4	1.4	0.6	-1.1	0.0	-0.6
6	0.2	0.5	-0.1	-5.3	1.8	2.8
7	-0.3	1.1	0.5	0.3	-0.2	7.1
8	-0.6	0.2	0.3	-0.8	-1.8	0.9
9	-0.1	0.5	0.3	8.2	-1.4	5.7
10	0.2	0.3	0.8	-1.9	-0.3	-2.6
MEAN	0.0	<b>0.5</b>	0.0	-0.7	-0.1	<b>2.0</b>
SD	0.3	<b>0.6</b>	0.7	3.5	1.0	<b>3.3</b>

**Table 2.** Interobserver differences in the safe screw angle measurements

#	Side	$\Theta$ ( ° )		$\Phi$ ( ° )	
		Inferior	Superior	Inferior	Superior
1	Left	-1.4	-2.0	0.8	-1.2
2	right	-1.5	1.2	-1.9	0.2
3	Left	1.9	-0.4	-1.6	-1.7
4	Left	-2.3	-0.7	4.7	2.8
5	Left	-0.8	1.3	0.6	0.0
6	Left	0.0	-1.9	0.5	-1.3
7	Left	2.0	-1.0	-0.1	-1.9
8	Left	-1.1	-1.2	4.7	-0.4
9	Right	0.0	-1.9	0.1	-0.5
10	Right	-0.5	-3.3	3.5	0.7
Mean		-0.4	<b>-1.0</b>	<b>1.1</b>	-0.3
SD		1.4	<b>1.4</b>	<b>2.4</b>	1.4

**Table 3.** Inferior and superior limits of the safe screw insertion direction

#	$\Theta$ ( $^{\circ}$ )		$\Phi$ ( $^{\circ}$ )	
	Inferior	Superior	Inferior	Superior
1	21.0	18.4	9.2	-7.0
2	11.3	9.1	5.3	-9.1
3	12.5	6.3	9.6	-13.7
4	19.1	17.7	6.0	-13.4
5	15.1	9.6	2.6	-16.1
6	13.2	5.9	17.3	1.4
7	22.9	21.0	13.3	-5.9
8	11.2	8.2	11.8	-10.0
9	16.0	12.9	13.1	-9.9
10	11.3	3.1	20.6	-1.8
11	20.0	17.3	0.3	-14.9
12	9.7	5.5	11.1	-5.1
13	21.8	19.4	8.0	-8.5
14	14.0	10.7	8.3	-13.5
15	17.6	14.7	9.3	-10.2
16	14.7	14.7	7.6	-5.7
17	9.6	2.8	9.6	-2.8
18	18.6	14.3	9.2	-6.1
19	8.9	5.4	16.7	-4.4
20	13.3	8.3	6.9	-10.1
Mean	15.1	11.3	9.8	-8.3
SD	4.3	5.7	4.8	4.6
Central angle	13.2 $\pm$ 4.9		0.7 $\pm$ 4.4	





**Stage I**  
Fixation of Calcaneal  
tuberosity and  
sustentaculum tali



**Stage II**  
Fixation of  
sustentaculum  
tali and shifted  
lateral fracture



**Fig. 1.** The lateral-to-medial screw insertion treatment for the Sanders Type II calcaneal fracture.

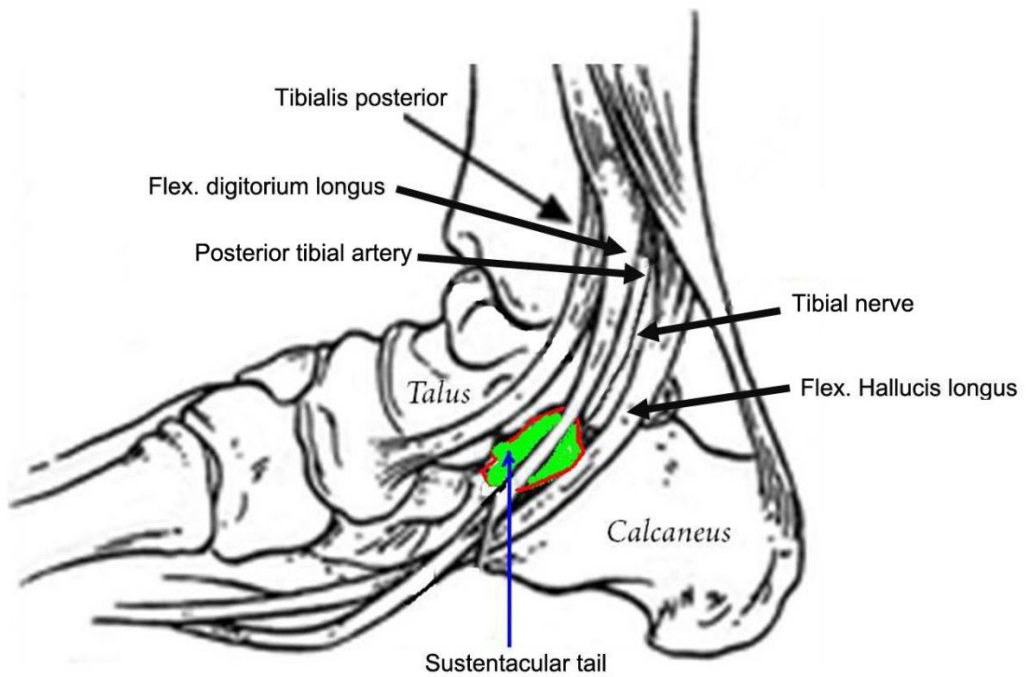


**Fig. 2.** Medial view of the ankle which shows complex structure.

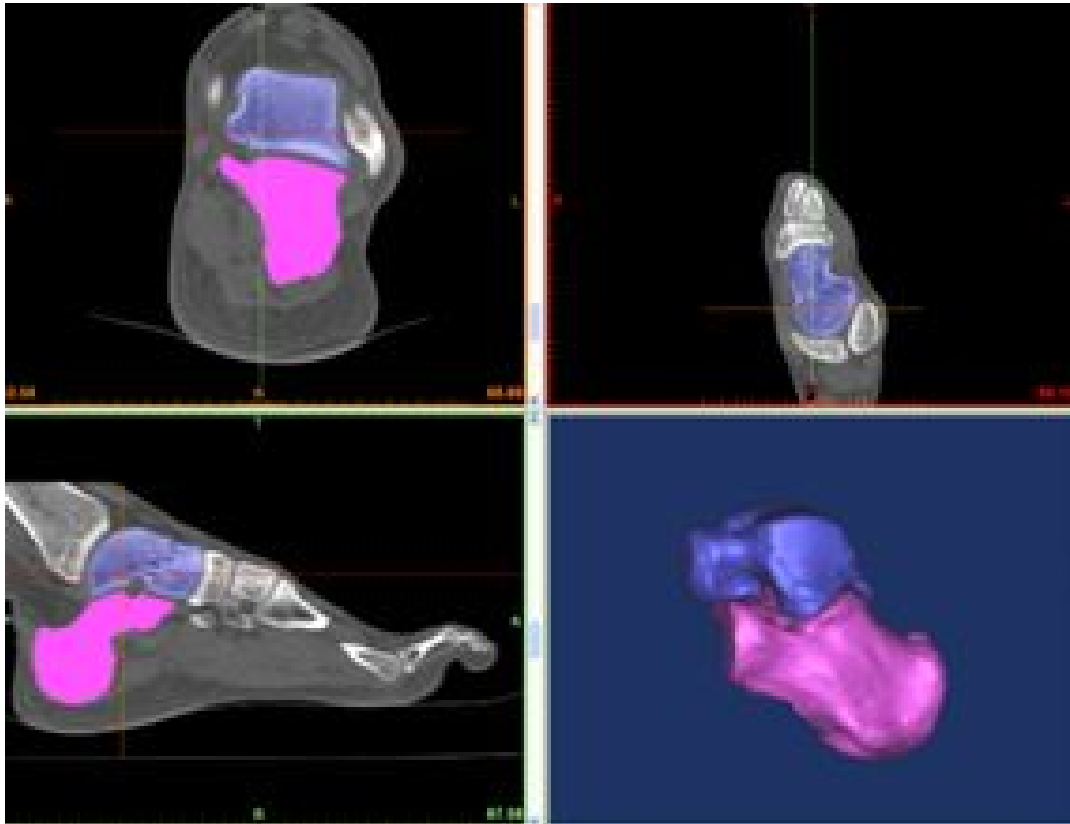


**Fig. 3.** The 3D polygon models of the talus and calcaneus.



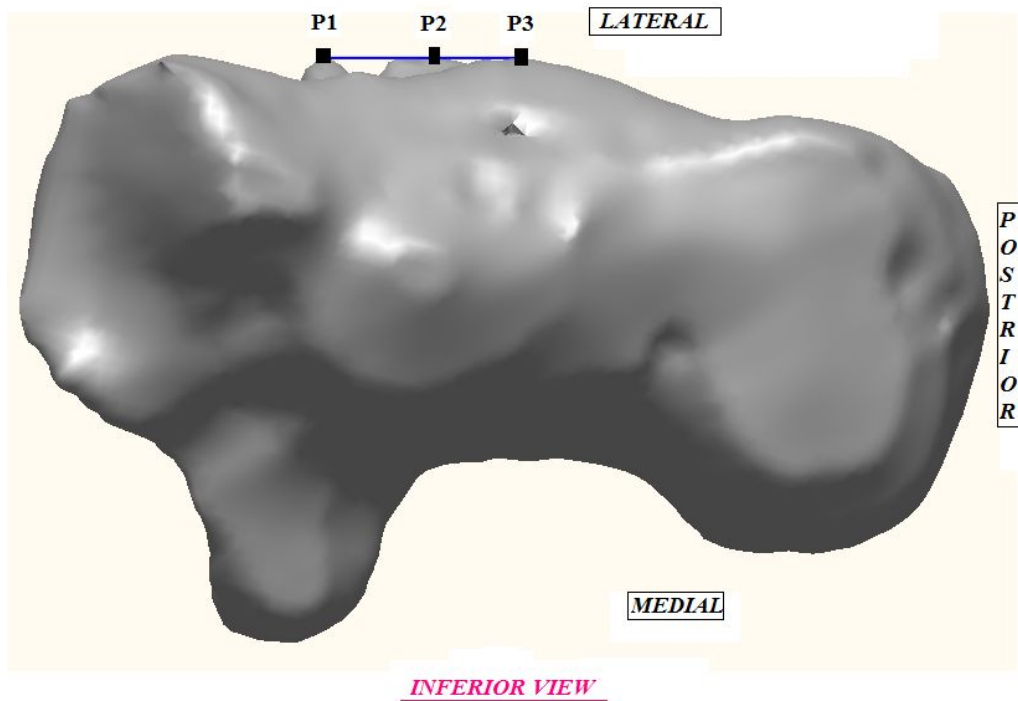


**Fig. 4.** Three prominent points were specified on the lateral calcaneal bony plane. Prominence was identified in the inferior view.

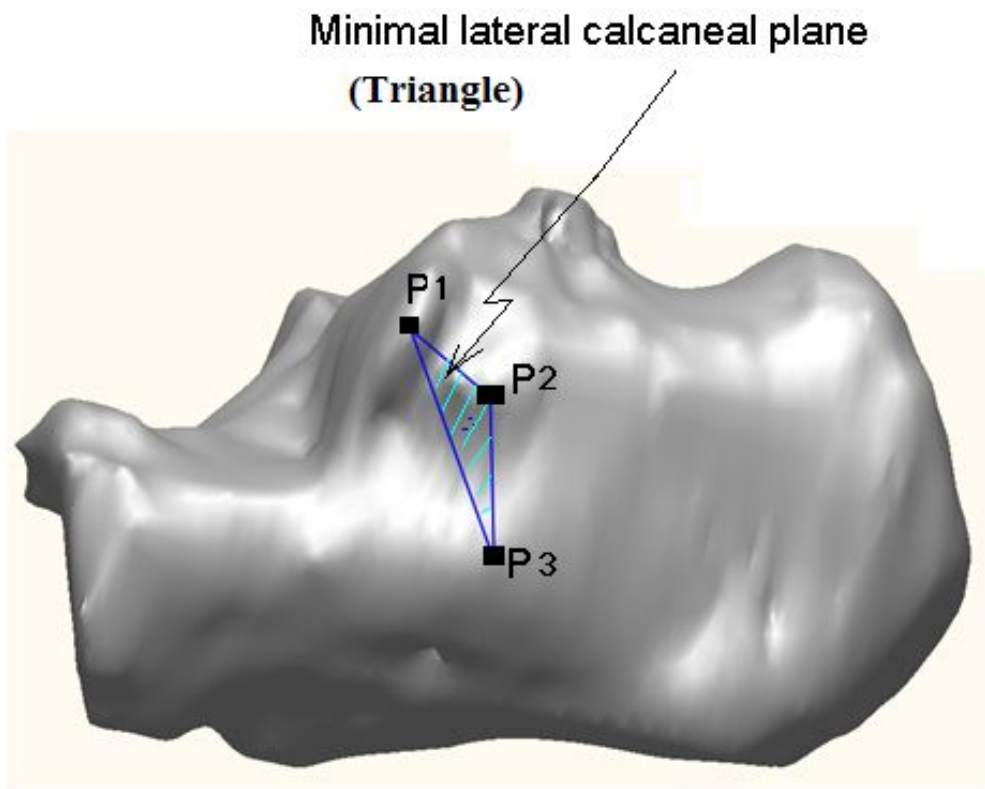


**Fig. 5.** The minimal lateral calcaneal plane was determined by the 3 prominent points on a small area near to talocalcaneal joint.

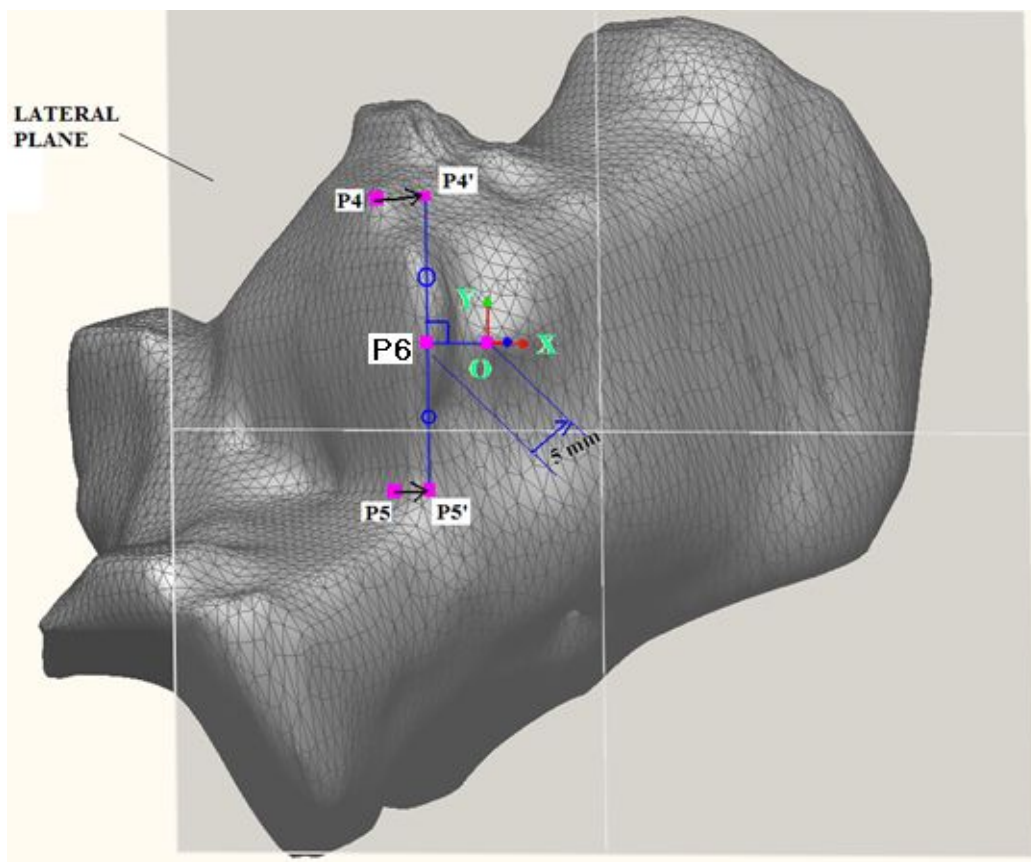


**Fig. 6.** Definition of the lateral calcaneal coordinate system

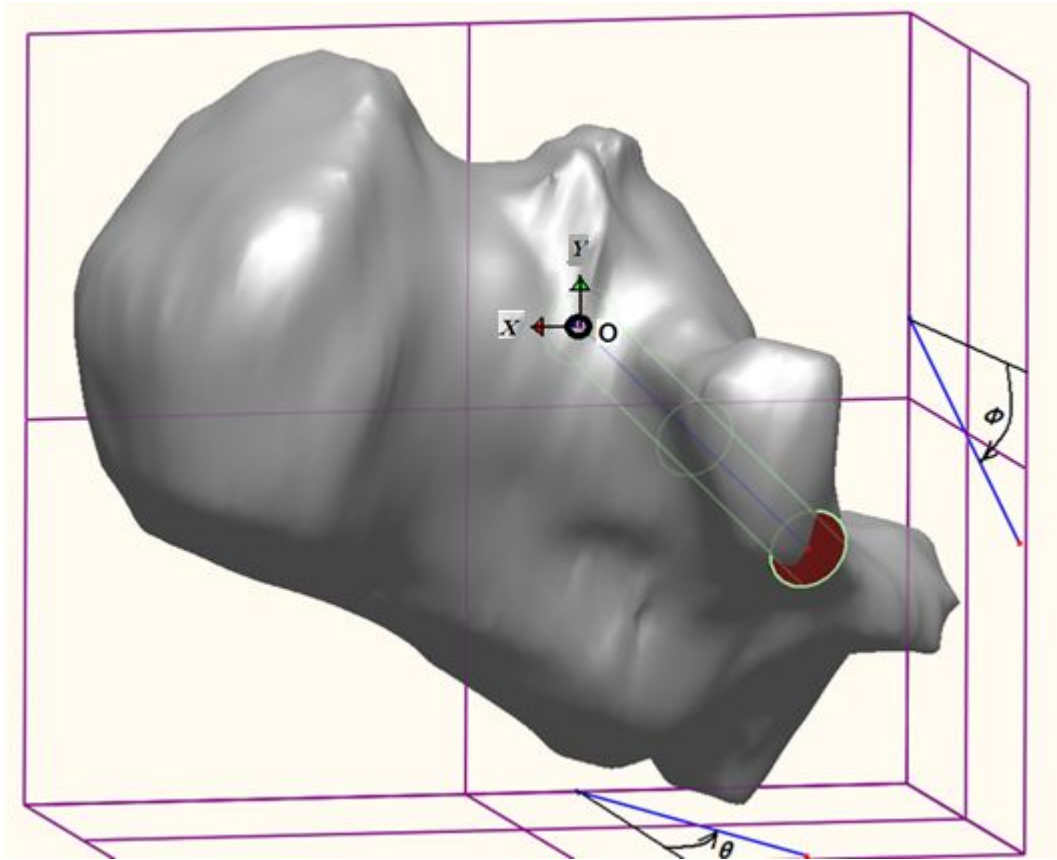


**Fig. 7.** The measured angles (  $\theta$  and  $\phi$  ) in the safe screw insertion simulation where the screw' s diameter was set as 6.5 mm.

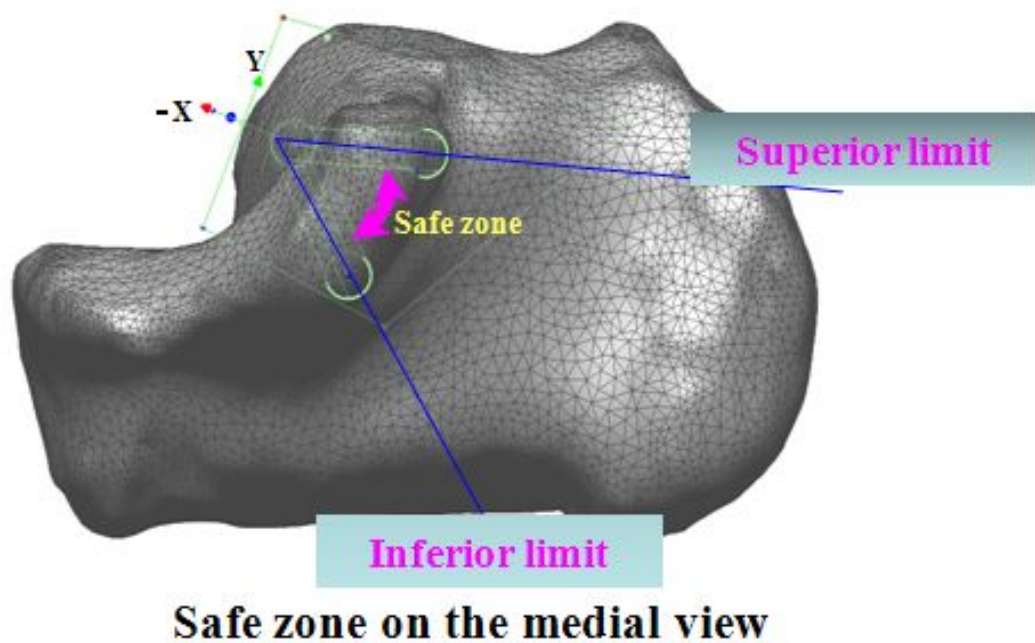


**Fig. 8.** Safe zone for the screw insertions the angle between the superior and inferior limits.

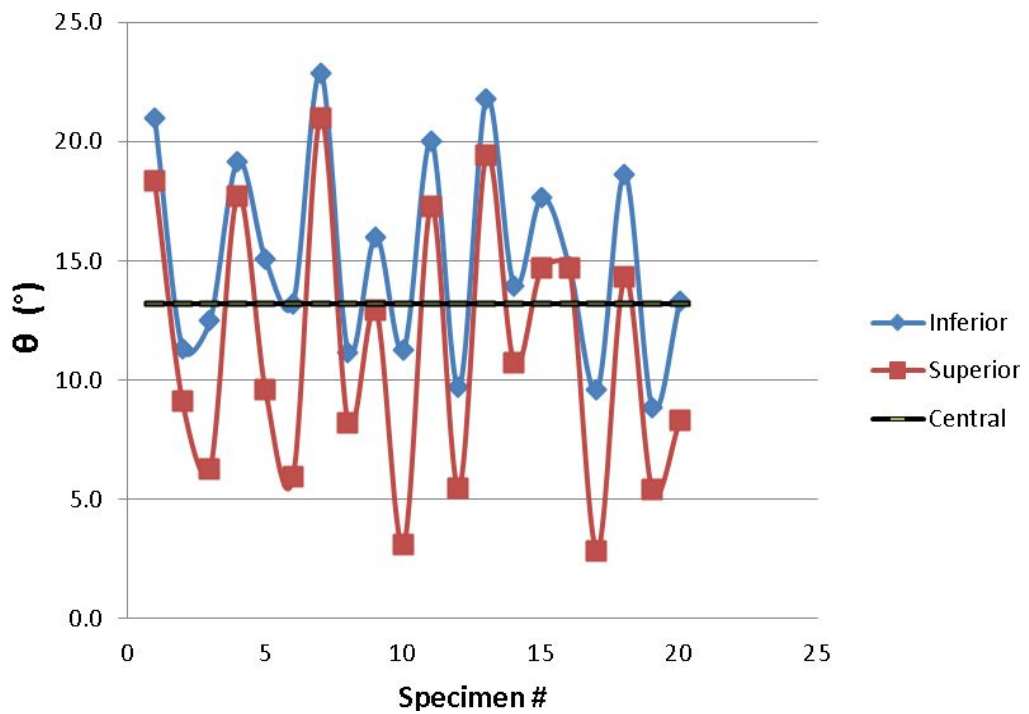


**Fig. 9.** Superior and inferior limits in the quasi-anteversion ( $\theta$ ) of the safe screw insertion direction

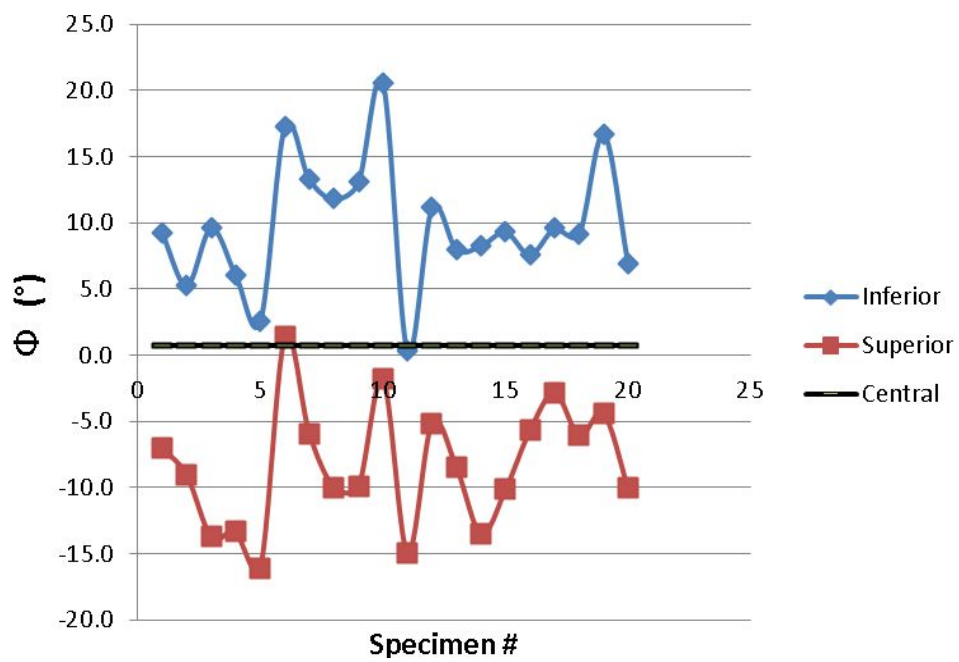


**Fig. 10.** Superior and inferior limits in the quasi-infraversion ( $\phi$ ) of the safe screw insertion direction.

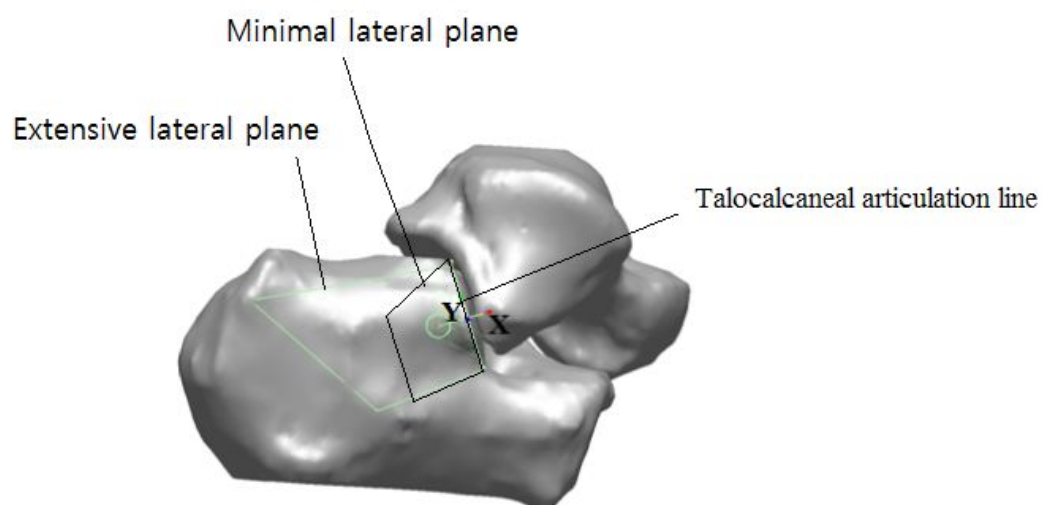


**Fig. 11.** A schematic comparison of the MIS lateral calcaneal plane and the extensive lateral calcaneal plane.